***The integration of food-grade starch into 3D printing technologies holds significant potential for creating customized, sustainable, and nutritionally enriched food products. This manuscript explores the development of novel sago starch-alginate food inks, specifically examining their rheological behavior, printability, and application potential for extrusion-based 3D food printing. Indonesia, holding over half the world's sago forests (1.28 million hectares), underutilizes this native staple. However, challenges persist in ensuring structural stability, reproducibility, and functional performance. The primary problem addressed is the identification of suitable hydrogel formulations that achieve both reliable printability and structural integrity post-printing. This study establishes that successful 3D printing of alginate-sago hydrogels requires a critical concentration threshold of 20% alginate/sago formulation. A notable feature is the significant discrepancy between theoretical rheological predictions and experimental outcomes for mid-range composites (e. g., Alg6/Sago6 and Alg8/Sago8), underscoring limitations in current rheological models. Sago starch, with its high amylose content and favorable shear-thinning behavior, offers superior printability and storage performance. While sago incorporation significantly enhances shear-thinning behavior and allows for effective viscosity modulation, storage modulus proved more predictive of printability than viscosity parameters. These findings provide practical insights for optimizing starch in maintaining structural fidelity. A circular and cubical shape of printing with height of 10 cm was reached using the line deposition of around 0.5 mm with 90% accuracy of design pattern***

***Keywords: 3D food printing, shear-thinning, storage modulus, native starch-alginate, sago starch***

UDC 664.015.5:541.64:006.91
DOI: 10.15587/1729-4061.2025.336896

# DEVELOPMENT OF SAGO STARCH-ALGINATE HYDROGELS FOR EXTRUSION-BASED 3D FOOD PRINTING

**Doohan Taqdissillah**
Master of Mechanical Engineering, Student*
**Muhammad Irsyad**
Master of Mechanical Engineering, Graduate*
**Yudan Whulanza**
*Corresponding author*
Doctor of Mechanical Engineering, Professor*
E-mail: yudan.whulanza@ui.ac.id
*Department of Mechanical Engineering
University of Indonesia
Margonda Raya, str. Pondok Cina, Kota Depok,
Jawa Barat, Indonesia, 16424

*Received 26.05.2025*
*Received in revised form 17.07.2025*
*Accepted date 05.08.2025*
*Published date 26.08.2025*

***How to Cite:*** *Taqdissillah, D., Irsyad, M., Whulanza, Y. (2025). Development of sago starch-alginate hydrogels for extrusion-based 3D food printing. Eastern-European Journal of Enterprise Technologies, 4 (11 (136)), 33–40. https://doi.org/10.15587/1729-4061.2025.336896*

## 1. Introduction

The application of 3D printing in the food industry has opened new possibilities in personalized nutrition, aesthetic food design, and efficient material usage. 3D food printing personalizes nutrition, customizing food with specific additives like vitamins, minerals, and proteins, to meet diverse dietary and health needs [1, 2]. 3D food printing efficiently uses diverse materials, like plant matter and by-products, creating high-value, customizable foods with less waste and improved shelf life [3]. Among various printable food biopolymers such as Xanthan gum [4], κ-carrageenan [5], Arabic gum [6], guar gum [7] and konjac gum [8] with their own benefit and specific objective.

Recently, starches have gained increasing attention due to their availability, cost-effectiveness, and gelling properties. As a significant source of carbohydrates in human nutrition, starch plays a crucial role in improving processed food quality [9]. Native starches such as sago, rice, and corn offer diverse structural and rheological characteristics, which can be tuned for layer-by-layer deposition.

This makes sago starch attract for 3D food printing due to its advantageous properties and abundant availability, particularly in Indonesia [10]. The 3D food printing technology allows for customized sago products, facilitating nutrient fortification to address deficiencies and potentially improving efficiency, reducing waste, and expanding market reach for this abundant local resource [11].

Despite its carbohydrate richness and food security potential, challenges like inefficient traditional processing, lack of protein/fat, and remote forest locations hinder its widespread use [12]. Therefore, research on the development and rheological characterization of sago starch-alginate hydrogels is highly relevant to advancing extrusion-based 3D food printing.

## 2. Literature review and problem statement

Sago starch's pseudoplastic (shear-thinning) behavior allows smooth extrusion from 3D printers, while its high storage modulus ensures rapid shape recovery and structural integrity. These rheological properties are critical for successful 3D printing, enabling strong stacking and dimensional stability. Its high amylose content further supports robust gel network formation [13].

Research about properties of sago starch was shown that native sago starch gels can be thick, necessitating adjustments, their inherent properties contribute to durable and elastic printed structures. Understanding and controlling factors like viscosity, yield stress, pseudoplasticity, and the effects of various additives and processing temperatures are

crucial for developing high-quality, printable food inks that meet desired structural [14].

While starch pastes offer valuable textural properties, there was an issue in their inherent susceptibility to retrogradation and syneresis often leads to undesirable shelf-life limitations and quality degradation. The reason for the issue is due to their water content, as the reassociation of starch molecules during cooling and storage can expel water from the gel network. Consequently, such pastes become prone to spoilage and exhibit textural changes, including increased hardness and reduced appeal [15].

A way to overcome that issue is mitigate these weaknesses lies in the incorporation of alginate, which can subsequently undergo ionic cross-linking with calcium chloride ($CaCl_2$). This cross-linking process creates a stable network, analogous to an eggshell-like structure, effectively preventing or significantly inhibiting both retrogradation and syneresis, thereby enhancing the stability and longevity of the material [16].

This approach was used in other common starches such as corn or potato starch, combining with alginate can further optimize its printability and expand its application in creating complex food designs. Blending starches with alginate enables rapid $Ca^{2+}$-induced crosslinking, reducing post-processing time and enhancing mechanical strength. In the case of corn starch, it demonstrated that hydrogels formulated with gelatinized high-amylopectin starch (GAP) exhibit significantly reduced retrogradation and syneresis compared to systems utilizing high-amylose starch, attributable to the branched molecular structure of amylopectin that impedes polymer reassociation [17]. Meanwhile, the potato starch revealed that alginate acts as a protective matrix for potato starch granules, effectively restricting granule swelling during gelatinization and reducing enzymatic hydrolysis by limiting α-amylase accessibility to starch substrates [18].

Yet, material-specific benchmarks for native sago-alginate systems remain unexplored, especially regarding Indonesia's abundant but underutilized sago resources. Addressing this gap is critical to unlocking their potential for cost-effective and sustainable food applications. This study aims to evaluate sago-alginate systems as promising candidates for developing tailored food inks in personalized nutrition.

Therefore, while the potential of 3D food printing for personalized nutrition and sustainable food production is recognized, there remains a critical research gap in fully understanding and optimizing novel, robust, and cost-effective food inks from underutilized local resources like sago. Specifically, further investigation is needed to precisely define the rheological criteria, including the interplay of viscosity and elastic modulus, that guarantee printability and post-printing structural integrity for sago-alginate composite hydrogels, thereby advancing their application in mass production of personalized food products [19, 20].

## 3. The aim and objectives of the study

The research aims to develop an alginate and sago-based hydrogel as an innovative hydrogel for 3D food printing. It explores the potential of biocompatible alginate and abundant Indonesian sago (with superior gelatinization and viscosity), expecting their combination to optimize rheological characteristics and structural stability for successful 3D food printing.

To achieve this aim, the following objectives are accomplished:

– to identify rheological characteristic for developing alginate and sago-based hydrogel to improve 3D food printing results;

– to investigate the effect of different concentrations of alginate and sago on the elastic modulus;

– to assess sago hydrogel printability on a 3D printer for desired culinary purpose.

## 4. Materials and methods

### 4. 1. The object and hypothesis of the study

The object of this study is the development and comprehensive rheological characterization of sago starch-alginate hydrogels specifically engineered for extrusion-based 3D food printing.

This study hypothesizes that combining sago starch's gelling and shear-thinning properties with alginate's rapid ionic cross-linking will yield superior printability and structural stability, enabling functional 3D food products from underutilized resources.

For this research, key assumptions include rheological characterization at a constant 25°C and evaluation of mechanical properties immediately post-printing for short-term stability.

A primary simplification is the use of a custom-built 3D extrusion printer, optimized for controlled conditions, though potential performance variations compared to commercial systems are acknowledged. This research, however, employs established methodologies in food rheology and 3D printing, applying specific optimizations and rigorous controls to ensure reliable evaluation of sago starch-alginate hydrogels for extrusion-based 3D food printing applications.

### 4. 2. Hydrogel solution and preparation

The hydrogel materials were formulated using food-grade sodium alginate (Sigma Aldrich, St. louis, USA) and sago flour (Metroxylon sagu, SAPAPUA, Papua, Indonesia). Three sample categories were prepared: alginate solutions, sago soultion (4%, 8% w/v denoted as Sago4, Sago8), and alginate-sago mixture.

Hydrogel solutions were prepared through a sequential protocol: sodium alginate was first dissolved in deionized water for 12 hours at 25°C. Sago flour was then incorporated at determined mass concentration under continuous mechanical stirring. The mixture was adjusted to the target volume with additional deionized water before heating to 80°C (± 2°C) with constant agitation. The samples were immediately cooled to room temperature and stored at 4°C for precisely 3 hours to enable network formation [21].

### 4. 3. Rheological observation

Starch solutions were prepared at 8%, 10%, and 12% (w/v) concentrations. Alginate was blended in a 1:1 ratio by weight with each starch. Solutions were heated to 80°C and cooled to 4°C for 3 hours before printing.

Rheological properties, including viscosity, elastic modulus (G′), and loss modulus (G″), were determined using industry-standard protocols on a Rheometer DHR1 (TA Instrument, New Castle, USA) to ensure comprehensive characterization of the hydrogel behavior. Measurements were performed on alginate solutions (Alg6, Alg8, Alg10), sago pastes (Sago4, Sago8), and alginate-sago mixture (Alg6/Sago6, Alg8/Sago8,

Alg10/Sago10). Hydrogel viscosity was measured at shear rates from 3 $S^{-1}$ to 117 $s^{-1}$. Moduli (G′ and G″) were measured as a function of angular frequency, from 0.628 rad/s to 628 rad/s. All measurements were conducted at 25°C.

### 4. 4. Printability assessment

This research used custom-developed 3D extrusion printer, designed to provide flexible and cost-effective material testing, was utilized to assess the printability of the hydrogels. This allowed for precise control over extrusion parameters relevant to food 3D printing, enabling detailed observation of fidelity ratio, line deposition, and shape retention.

Printability was assessed by designing 3D models using CAD software (AutoCAD), converting them with CAM software (Candle GRBL controller application), and printing them with our 3D extrusion printer and prepared hydrogels. Post-printing results were observed and evaluated for each hydrogel variation (Image J apps). A multi-layer grid model was used to assess filament width, consistency, pore dimensions, layer integrity, and deposition merging [22].

An Arduino Uno microcontroller controlled the X, Y, and Z axes using Grbl code. An Arduino Nano controlled a 2 RPM DC motor for the extruder. Mechanical parts like the syringe plunger, holder, and DC motor mount were printed with PLA filament. Grbl is open-source software for 3-axis CNC machines (X, Y, Z), executable on Arduino boards. The printer was operated using open-source Candle software (version 1.1.7). Manual normalization of needle/nozzle coordinates was done via Candle. G-code commands were then sent to initiate printing.

For speed parameters, movements along x, y, and z axes were restricted to 500 mm/minute (8.33 mm/second) due to motor limitations. Simplify3D-generated G-code could not be directly executed due to the printer's simpler CNC firmware. A G-code generator from cnc-apps.com was used to remove extraneous commands (e. g., "E" for extruder). The revised G-code was loaded into Candle, requiring manual nozzle coordinate normalization before printing.

### 4. 5. Stability testing

Printed samples were stored at 25°C and 4°C. Moisture content and structure height were measured over 72 hours.

## 5. Results of develop an alginate and sago-based hydrogel for 3D food printing

### 5. 1. Rheological characteristic of sago alginate

Fig. 1, *a* display the comparation between Alginate, sago and alginate-sago in 8% concentration, Fig. 1, *b–d* displays the apparent viscosity of every concentration for Alginate, sago and alginate-sago. Viscosity showed that sago-based formulations shown higher viscosity and strong shear-thinning behavior, it means sago starch is suitable for extrusion.

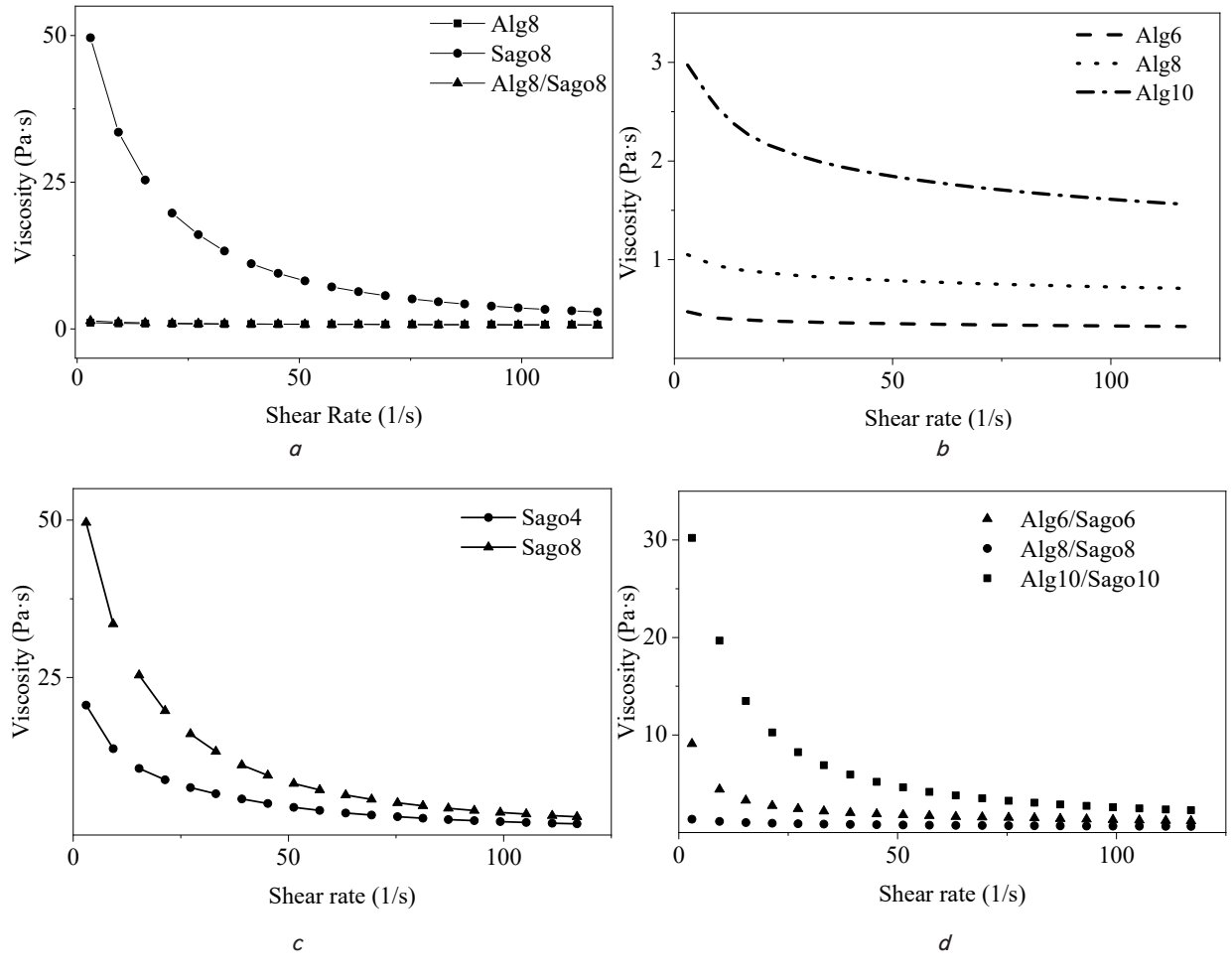


Fig. 1. Viscosity value in different food ink: *a* — comparation of hydrogel; *b* — alginate; *c* — sago; *d* — alginate-sago

Molecular interactions fundamentally explain these rheological behaviors. Sago starch's high amylose content (21.4 to 30%, Table 2) enables robust double-helical associations during gelatinization but also drives retrogradation. Alginate counters this through dual mechanisms: hydrogen bonding with leached amylose chains restricts molecular mobility (Fig. 2) [13]. This synergy produces the pronounced shear-thinning observed, where amylose-alginate complexes align under shear stress during extrusion, then rapidly re-entangle after deposition to restore structural integrity [13, 16]. The failure of mid-range composites such as Alg8/Sago8 stems from insufficient alginate to fully suppress retrogradation while inadequate amylose leaching weakens network formation [17].

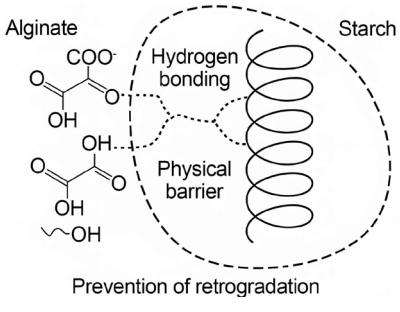


Fig. 2. Molecular mechanism of calcium-mediated 'egg-box' cross-linking in sago-alginate hydrogels

Fig. 1 also displays the viscosity behavior of alginate, sago, and alginate-sago hydrogels. Fig. 1, *a* graph shows that increasing alginate concentration (Alg6, Alg8, Alg10) leads to higher viscosity, with Alg10 exhibiting the highest. Fig. 1, *b* graph demonstrates a similar trend for sago starch, where Sago8 has a higher viscosity than Sago4. Both sets of single-component graphs indicate shear-thinning behavior, as viscosity decreases with the increasing shear rate. Fig. 1, *c* graph, featuring alginate-sago mixtures (Alg6/Sago6, Alg8/Sago8, Alg10/Sago10), also shows pronounced shear-thinning, with viscosity generally increasing with higher total solid content. Notably, the Alg10/Sago10 mixture exhibits significantly higher viscosity across all shear rates compared to the other combinations. Finally, Fig. 1, *d* bar chart directly compares the viscosity at a shear rate of 50 1/s, indicating that 8% Sago possesses the highest viscosity among 8% Alginate, 8% Sago, and 8% Alg-Sago (likely meaning a combined 8% total solids). This comprehensive view highlights how composition and concentration influence the rheological properties crucial for applications like 3D printing.

### 5. 2. The correlation of concentration and elastic modulus

Fig. 3, *a–c* displays the apparent storage/loss modulus of every concentration for Alginate, sago and alginate-sago. Sago-alginate exceeds elastic threshold (250 Pa) that make this solution can maintain excellent elastic properties.

The image presents four graphs detailing the storage and loss moduli of alginate, sago, and alginate-sago hydrogels. Graphs A (Alg6), B (Sago4), and C (Alg6/Sago6) all show similar trends: the storage modulus ($G'$) consistently higher than the loss modulus ($G''$) across increasing angular frequencies. This indicates a predominantly elastic, solid-like behavior, essential for structural integrity in materials like hydrogels used in 3D printing. As angular frequency increases, both moduli rise, with the storage modulus showing a more significant increase, signifying a strengthening of the gel structure under applied stress. Graph D, a bar chart, specifically compares the storage and loss moduli at an angular frequency of 396 rad/s for 6% Alginate-Sago, 4% Sago, and 6% Alginate. It clearly illustrates that the storage modulus (orange bars) is substantially higher than the loss modulus (blue bars) for all formulations, reinforcing their gel-like characteristics. Notably, 4% Sago exhibits the highest storage modulus among the three at this specific frequency, suggesting a more rigid structure. This data is critical for understanding the viscoelastic properties and printability of these hydrogel formulations.

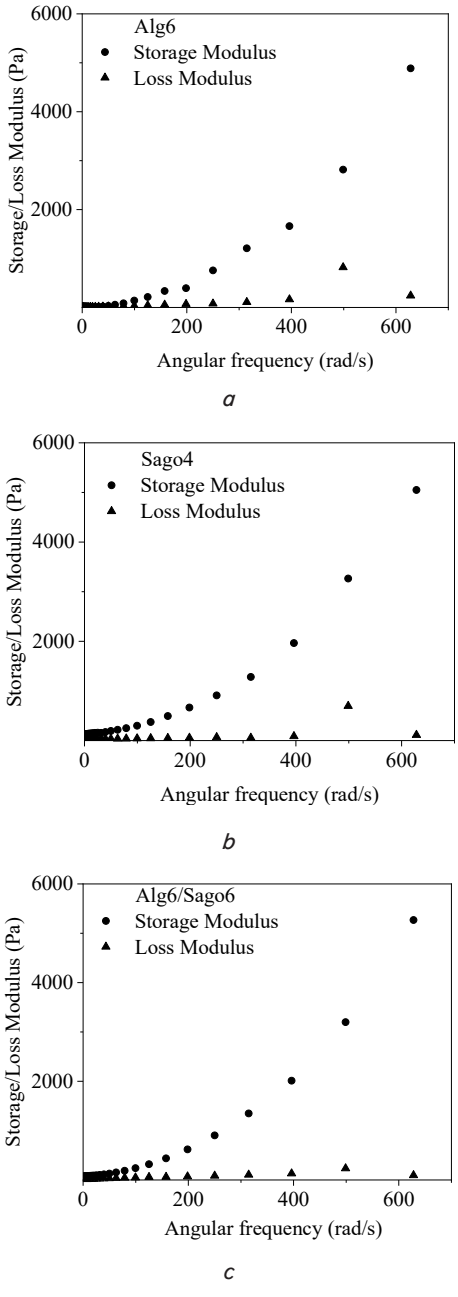


Fig. 3. Storage/loss modulus value in different food ink: *a* – alginate; *b* – sago; *c* – sago-alginate

### 5. 3. Sago hydrogel printability on a 3D printer

Experimental validation revealed a critical concentration threshold: only the Alg10/Sago10 composite (20% total solids) produced structurally stable 3D prints (Fig. 4), maintaining

dimensional accuracy in both grid patterns and cylindrical towers. Lower-concentration formulations (Alg6/Sago6, Alg8/Sago8) exhibited immediate collapse post-extrusion despite favorable viscosity profiles (15–25 Pa·s). This outcome directly correlates with Alg10/Sago10's storage modulus ($G'$ = 320 Pa at 1 rad/s), which exceeded the 250 Pa stability threshold established in prior studies [23]. The ideal viscosity range of 0.3–30 Pa·s might not be sufficient; a different study used a different material (gelatin) and did not measure modulus parameters [24].

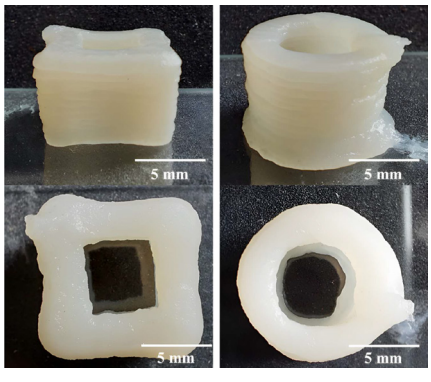


Fig. 4. 3D printing results of 10% alginate-sago

Even small amounts of gelatin could significantly increase storage modulus due to better molecular bonding. A study using rice starch with high storage modulus values showed successful solid prints, though their focus was food printing with starch as the dominant material over alginate. Comparative analysis suggests storage modulus significantly predicts successful hydrogel printability. The discrepancy between predicted and actual printability might also be due to technical issues during measurement, like procedural deviations or equipment condition [25].

Table 1

Result of alginate-sago layer deposition during printing

| Parameter | Geometry | Designed | Realized | Stdev | Margin gap (mm) | Margin gap (%) | Accuracy (%) |
|---|---|---|---|---|---|---|---|
| Width of layer deposition (mm) | Cubic vase | 0.8 | 3.20 | 0.03 | 2.4 | 300.00 | –200.00 |
| | Cylindrical vase | 0.8 | 2.80 | 0.13 | 2 | 250.00 | –150.00 |
| Height of layer deposition (mm) | Cubic vase | 0.8 | 0.86 | 0.05 | 0.06 | 7.50 | 92.50 |
| | Cylindrical vase | 0.8 | 0.82 | 0.04 | 0.02 | 2.50 | 97.50 |
| Height overall dimension (total 10 layers) | Cubic vase | 8 | 8.32 | 0.18 | 0.32 | 4.00 | 96.00 |
| | Cylindrical vase | 8 | 8.15 | 0.15 | 0.15 | 1.88 | 98.13 |

Table 1 reveals significant dimensional deviations in layer width (200% over-extrusion in cubic vase vs. 150% in cylinder), contrasting with height accuracy (96–98.13%). This discrepancy stems from two key factors. First, nozzle kinematics during rectilinear paths (cubic vase) cause localized material accumulation at corners due to deceleration coupled with uninterrupted extrusion—a direct consequence of the absence of retraction capability. Conversely, continuous curvilinear motion (cylinder) minimizes this accumulation effect. Second, the exceptional height fidelity is attributed to the rapid structural recovery of hydrogel ($G' > G''$), where subsequent nozzle layers vertically shear excess material during deposition. This shearing mechanism aligns the printed height with the designed dimensions and is consistent with the observed shear-thinning recovery behavior.

Table 2 shown sago starch [26] compared to other starches, sago's molecular profile offers distinct advantages.

Table 2

Comparations of sago, corn and potato starch

| Properties | Sago | Corn | Potato | References |
|---|---|---|---|---|
| Starch content (%) | 80–87 | 93.76 | 84.82 | [27] |
| Amylose content (%) | 21.4–30 | 13.35 | 11.67 | [27] |
| Granule size (μm) | 37.59 | 5–18 | 15–45 | [28, 29] |
| Gelatinization temperature (°C) | 68–90 | 59–68 | 55–62 | [30, 31] |
| Retrogradation tendency | High | Medium | Low | [17, 18] |

Corn starch's low amylose content (13.35%) limits network strength, yielding poor shape fidelity despite reduced syneresis [17], while potato starch's excessive granule swelling creates brittle gels prone to fracture during printing [18]. Sago's moderate amylose level achieves an optimal balance: its interaction with alginate through hydrogen bonding avoids the rigidity of potato-based gels and the weakness of corn-based systems [13].

## 6. Discussion of rheological properties and printability outcomes

The experimental outcomes demonstrate that successful printability and structural fidelity are governed by the complex interplay between rheological properties and molecular interactions. While all formulations exhibited essential shear-thinning behavior (Fig. 1, *c*), enabling smooth extrusion, only the Alg10/Sago10 composite (20% total solids) achieved structural stability (Fig. 4) due to its storage modulus ($G'$ = 320 Pa) surpassing the critical 250 Pa threshold [23].

The storage modulus analysis in Fig. 2 revealing how different concentrations influence the elastic properties of the hydrogels. The results show that all tested formulations (Alg6, Sago4, and Alg6/Sago6) consistently exhibit elastic dominance ($G' > G''$), a fundamental characteristic for shape retention. This is a direct consequence of the formation of a robust gel network. However, the data also highlights key differences in network strength while pure alginate and pure sago both show significant elastic behavior, the composite Alg6/Sago6 maintains a substantial $G'$ (>100 Pa) even at a lower total solids content, suggesting molecular-level synergy. Fig. 2 also revealing that storage modulus is the primary predictor of structural integrity than viscosity. The observed fidelity discrepancies (Table 1), where curvilinear paths (cylinder) showed superior accuracy to rectilinear paths (cube), further highlight the role of rapid elastic recovery ($G' > G''$) in maintaining dimensional stability after deposition, while uninterrupted extrusion during kinematic transitions caused localized material accumulation.

When compared to other starches, sago's molecular profile presents a comparative analysis of key properties. Sago starch is characterized by a starch content of 80–87% and a notably high amylose content, ranging from 21.4–30%, which is significantly greater than both corn (13.35%) and potato (11.67%) starches. Sago starch also exhibits a larger average granule size

of 37.59 μm, compared to corn (5–18 μm) and potato (15–45 μm) starches, though the range overlaps [28, 29]. The gelatinization temperature for sago starch (68–90°C) is higher than that of corn and potato starches, which fall in the 59–68°C and 55–62°C ranges, respectively. Furthermore, sago starch shows a high tendency for retrogradation, contrasting with the medium retrogradation of corn and the low retrogradation of potato starch. These distinct properties highlight why sago starch's behavior differs from other common starches in food applications [17, 18] (Table 2). This molecular compatibility enables sago-alginate composites to maintain the shear-thinning necessary for extrusion while developing the elastic modulus critical for layer stacking, a balance unattainable with other starches at equivalent concentrations. In contrast, corn and potato starches have different compositions, smaller granule sizes, and generally lower gelatinization temperatures and retrogradation tendencies. These variations in properties, particularly the higher amylose content and retrogradation of sago, are critical for understanding their functional differences in food product development.

Alginate's concentration-dependent functionality ultimately underpins the hydrogel's performance. At 10% concentration, alginate achieves three critical effects: sufficient ionic cross-linking density to exceed the $G'$ stability threshold, physical immobilization of water molecules that reduces syneresis compared to pure sago gels [16], and suppression of amylose recrystallization through hydrogen bonding. This multifunctional role transforms sago from a retrogradation-prone starch into a printable biomaterial, where optimized chain entanglement enables shear-thinning during extrusion while cross-linking ensures elastic recovery after deposition. These mechanisms establish sago-alginate as a sustainable platform for nutrient-dense food printing.

This study establishes that sago starch's rheological characteristics, including pseudoplastic behavior and high storage modulus, are critical for successful 3D printing, ensuring good extrudability and shape retention. Despite these advantages, several limitations must be acknowledged. First, the experiments were conducted under controlled laboratory conditions using a custom-built extrusion printer, which may not fully replicate the complexities of commercial food printing systems. Second, while the study focused on short-term stability and immediate post-printing structure, it did not include a comprehensive evaluation of long-term shelf life or microbial safety over extended storage.

Future research should aim to validate these findings across broader environmental and operational conditions. It is indicated that starch pastes face issues like retrogradation and syneresis, which compromise shelf-life. To address this, incorporating alginate creates a stable, eggshell-like network via calcium chloride cross-linking, inhibiting these degradation processes and enhancing material stability. This approach provides a solution for developing durable, printable food inks from sago starch. Finally, exploring the integration of bioactive compounds, proteins, or fortification ingredients will expand the functional scope of sago-alginate inks for personalized and nutritionally enriched food systems.

## 7. Conclusion

1. To identify optimal rheological characteristics for developing alginate and sago-based hydrogels, this study confirmed that all tested formulations, including pure Alginate, Sago, and their composites (Alg6/Sago6, Alg8/Sago8, Alg10/Sago10), consistently exhibited prominent shear-thinning behavior across shear rates from 3 to 117 $s^{-1}$. This crucial rheological property ensures low viscosity during extrusion through the nozzle, facilitating smooth material flow critical for extrusion-based 3D food printing.

2. Regarding the optimization of storage and loss modulus values for consistent printing, it was found that the storage modulus ($G'$) consistently remained higher than the loss modulus ($G''$) across all observed formulations and angular frequencies (0.628 to 628 rad/s). This dominant elastic behavior is essential for hydrogels to retain their shape and structural integrity post-extrusion. Notably, the Alg10/Sago10 formulation achieved a G′ of approximately 320 Pa at 1 rad/s, surpassing the critical 250 Pa threshold necessary for stable self-supporting structures.

3. In assessing hydrogel printability for desired culinary purposes, experimental validation revealed a critical concentration threshold: only the Alg10/Sago10 composite, with 20% total solids, successfully produced structurally stable 3D prints, reveals significant dimensional deviations in layer width (200% over-extrusion in cubic vase vs. 150% in cylinder), contrasting with height accuracy (96–98.13%). Lower concentration composites (Alg6/Sago6, Alg8/Sago8) consistently failed to retain their shape and collapsed immediately post-extrusion, despite exhibiting viscosity profiles that might theoretically appear favorable. This significant discrepancy underscores that while viscosity is important, storage modulus proved to be a more reliable and predictive parameter for successful printability than viscosity parameters alone. These findings provide practical insights for optimizing starch-alginate hydrogels to achieve high structural fidelity in 3D food printing, particularly for nutritional applications where desired solid content can be precisely controlled.

## Conflict of interest

The authors declare that they have no known competing financial interests or personal relationships that could have appeared to influence the work reported in this paper.

## Financing

The study was provided by Graduate Program Research Grant Ministry of Education of Indonesia 2024 No. NKB-971/UN2.RST/HKP.05.00/2024.

## Data availability

Data will be made available on reasonable request.

## Use of artificial intelligence

The authors have used artificial intelligence technologies within acceptable limits to provide their own verified data, which is described in the research methodology section.

## Acknowledgments

Grant Reverse Engineering 2024/2025 Faculty of Engineering Universitas Indonesia.

References


1. Whulanza, Y., Arsyan, R., Saragih, A. S. (2018). Characterization of hydrogel printer for direct cell-laden scaffolds. AIP Conference Proceedings. https://doi.org/10.1063/1.5023972
2. Sun, J., Zhou, W., Yan, L., Huang, D., Lin, L. (2018). Extrusion-based food printing for digitalized food design and nutrition control. Journal of Food Engineering, 220, 1–11. https://doi.org/10.1016/j.jfoodeng.2017.02.028
3. Shen, D., Zhang, M., Mujumdar, A. S., Li, J. (2023). Advances and application of efficient physical fields in extrusion based 3D food printing technology. Trends in Food Science & Technology, 131, 104–117. https://doi.org/10.1016/j.tifs.2022.11.017
4. Habibi, H., Khosravi-Darani, K. (2017). Effective variables on production and structure of xanthan gum and its food applications: A review. Biocatalysis and Agricultural Biotechnology, 10, 130–140. https://doi.org/10.1016/j.bcab.2017.02.013
5. Udo, T., Mummaleti, G., Mohan, A., Singh, R. K., Kong, F. (2023). Current and emerging applications of carrageenan in the food industry. Food Research International, 173, 113369. https://doi.org/10.1016/j.foodres.2023.113369
6. Tahir, H. E., Xiaobo, Z., Mahunu, G. K., Arslan, M., Abdalhai, M., Zhihua, L. (2019). Recent developments in gum edible coating applications for fruits and vegetables preservation: A review. Carbohydrate Polymers, 224, 115141. https://doi.org/10.1016/j.carbpol.2019.115141
7. Mudgil, D., Barak, S., Khatkar, B. S. (2011). Guar gum: processing, properties and food applications – A Review. Journal of Food Science and Technology, 51 (3), 409–418. https://doi.org/10.1007/s13197-011-0522-x
8. Yang, D., Yuan, Y., Wang, L., Wang, X., Mu, R., Pang, J. et al. (2017). A Review on Konjac Glucomannan Gels: Microstructure and Application. International Journal of Molecular Sciences, 18 (11), 2250. https://doi.org/10.3390/ijms18112250
9. Cui, Y., Li, C., Guo, Y., Liu, X., Zhu, F., Liu, Z. et al. (2022). Rheological & 3D printing properties of potato starch composite gels. Journal of Food Engineering, 313, 110756. https://doi.org/10.1016/j.jfoodeng.2021.110756
10. Ehara, H., Toyoda, Y., Johnson, D. V. (Eds.) (2018). Sago Palm. Springer Singapore. https://doi.org/10.1007/978-981-10-5269-9
11. Sumardiono, S., Rakhmawati, R. B. (2017). Physicochemical Properties of Sago Starch Under Various Modification Process: An Overview. Advanced Science Letters, 23 (6), 5789–5791. https://doi.org/10.1166/asl.2017.8833
12. Whulanza, Y., Azadi, A., Supriadi, S., Rahman, S. F., Chalid, M., Irsyad, M. et al. (2022). Tailoring mechanical properties and degradation rate of maxillofacial implant based on sago starch/polylactid acid blend. Heliyon, 8 (1), e08600. https://doi.org/10.1016/j.heliyon.2021.e08600
13. Yoon, Y., Kim, C. H., Lee, J. E., Yoon, J., Lee, N. K., Kim, T. H., Park, S.-H. (2019). 3D bioprinted complex constructs reinforced by hybrid multilayers of electrospun nanofiber sheets. Biofabrication, 11 (2), 025015. https://doi.org/10.1088/1758-5090/ab08c2
14. Hirao, K., Kondo, T., Kainuma, K., Takahashi, S. (2021). Starch gel foods in cookery science: application of native starch and modified starches. Journal of Biorheology, 35 (1), 29–41. https://doi.org/10.17106/jbr.35.29
15. Li, C. (2024). Unraveling the Complexities of Starch Retrogradation: Insights from Kinetics, Molecular Interactions, and Influences of Food Ingredients. Food Reviews International, 40 (9), 3159–3182. https://doi.org/10.1080/87559129.2024.2347467
16. Wang, S., Li, C., Copeland, L., Niu, Q., Wang, S. (2015). Starch Retrogradation: A Comprehensive Review. Comprehensive Reviews in Food Science and Food Safety, 14 (5), 568–585. https://doi.org/10.1111/1541-4337.12143
17. Feltre, G., Almeida, F. S., Sato, A. C. K., Dacanal, G. C., Hubinger, M. D. (2020). Alginate and corn starch mixed gels: Effect of gelatinization and amylose content on the properties and in vitro digestibility. Food Research International, 132, 109069. https://doi.org/10.1016/j.foodres.2020.109069
18. Ramírez, C., Millon, C., Nuñez, H., Pinto, M., Valencia, P., Acevedo, C., Simpson, R. (2015). Study of effect of sodium alginate on potato starch digestibility during in vitro digestion. Food Hydrocolloids, 44, 328–332. https://doi.org/10.1016/j.foodhyd.2014.08.023
19. Zhong, Q., Chen, Y., Zhang, X., Yang, G., Jin, W., Peng, D., Huang, Q. (2024). Correlation between 3D printability and rheological properties of biopolymer fluid: A case study of alginate-based hydrogels. Journal of Food Engineering, 370, 111970. https://doi.org/10.1016/j.jfoodeng.2024.111970
20. Ji, H., Zhao, J., Chen, J., Shimai, S., Zhang, J., Liu, Y. et al. (2022). A novel experimental approach to quantitatively evaluate the printability of inks in 3D printing using two criteria. Additive Manufacturing, 55, 102846. https://doi.org/10.1016/j.addma.2022.102846
21. Cui, Y., Yang, F., Wang, C., Blennow, A., Li, C., Liu, X. (2024). 3D Printing windows and rheological properties for normal maize starch/sodium alginate composite gels. Food Hydrocolloids, 146, 109178. https://doi.org/10.1016/j.foodhyd.2023.109178
22. Yang, F., Zhang, M., Bhandari, B. (2015). Recent development in 3D food printing. Critical Reviews in Food Science and Nutrition, 57 (14), 3145–3153. https://doi.org/10.1080/10408398.2015.1094732
23. Whulanza, Y., Hidayaturrahmi, P., Kurniawati, T., AJ, R. (2017). Realization and testing of multi-material 3D printer for bone scaffold fabrication. AIP Conference Proceedings, 1817, 040001. https://doi.org/10.1063/1.4976786
24. Fonkwe, L. G., Narsimhan, G., Cha, A. S. (2003). Characterization of gelation time and texture of gelatin and gelatin–polysaccharide mixed gels. Food Hydrocolloids, 17 (6), 871–883. https://doi.org/10.1016/s0268-005x(03)00108-5
25. Yan, N., Yang, L., Xiao, X., Huang, P., Shu, C., Song, S., Tan, H. (2025). Research on Structural–Mechanical Property of Rice Starch Gels for Food 3D Printing and Flexible Sensing. Journal of Food Process Engineering, 48 (5). https://doi.org/10.1111/jfpe.70126
26. Okazaki, M. (2018). The Structure and Characteristics of Sago Starch. Sago Palm, 247–259. https://doi.org/10.1007/978-981-10-5269-9_18

27. Du, C., Jiang, F., Jiang, W., Ge, W., Du, S. (2020). Physicochemical and structural properties of sago starch. International Journal of Biological Macromolecules, 164, 1785–1793. https://doi.org/10.1016/j.ijbiomac.2020.07.310
28. Nishiyama, S., Okazaki, M., Katsumi, N., Honda, Y., Tsujimoto, M. (2015). Surface charge on sago starch granules. Sago Palm, 23 (2), 77–83. Available at: https://www.sagopalmsociety.com/_files/ugd/3f58e5_4142a53f161840f68dc865bd28bed78f.pdf
29. Singh, J., Singh, N. (2003). Studies on the morphological and rheological properties of granular cold water soluble corn and potato starches. Food Hydrocolloids, 17 (1), 63–72. https://doi.org/10.1016/s0268-005x(02)00036-x
30. Pérez, E. E., Breene, W. M., Bahnassey, Y. A. (1998). ariations in the Gelatinization Profiles of Cassava, Sagu and Arrowroot Native Starches as Measured with Different Thermal and Mechanical Methods. Starch - Stärke, 50 (2-3), 70–72. https://doi.org/10.1002/(sici)1521-379x(199803)50:2/3<70::aid-star70>3.0.co;2-u
31. Ronda, F., Roos, Y. H. (2008). Gelatinization and freeze-concentration effects on recrystallization in corn and potato starch gels. Carbohydrate Research, 343 (5), 903–911. https://doi.org/10.1016/j.carres.2008.01.026